(1)

23(1)

気象庁欧文海洋報告

第23巻 第1号

THE OCEANOGRAPHICAL MAGAZINE

Vol. 23 No. 1

CONTENTS

TSUCHIDA, T.: On the seasonal variation of the Kuroshio southeast of Yakushima Island 1

MORIYASU, S.: On the change of monthly sea surface temperature in the Western North Pacific (III) 11

OHWADA, M.: Distribution of chlorophyll and phaeophytin in the Sea of Japan 21

NAGASAKA, K.: An STD system for instrumented buoy 33

LIBRARY
MAR 31 1972
FISH & WILDLIFE SERVICE

Published by the Japan Meteorological Agency

December, 1971

The Oceanographical Magazine
Vol. 23, No. 1, pp. 1 to 10, December 1971

On the seasonal variation of the Kuroshio southeast of Yakushima Island

Takeo TSUCHIDA

Nagasaki Marine Observatory

(Received June 21, 1971)

Abstract: A special project for CSK was carried out from May 1965 to February 1968 for study of the seasonal variation of the Kuroshio across a section southeast of Yakushima Island on board the R/V *Chofu-maru* and *Shumpu-maru* belonging to the Japan Meteorological Agency. Hydrographic section was made 24 times during those three years.

The high-velocity zone seems to be higher in speed from spring to early fall.

Seasonal variations of water temperature and salinity are large in the surface-mixed layer and very small in the Subtropical Mode Water.

1. Introduction

In order to monitor the seasonal variation of the Kuroshio flowing into

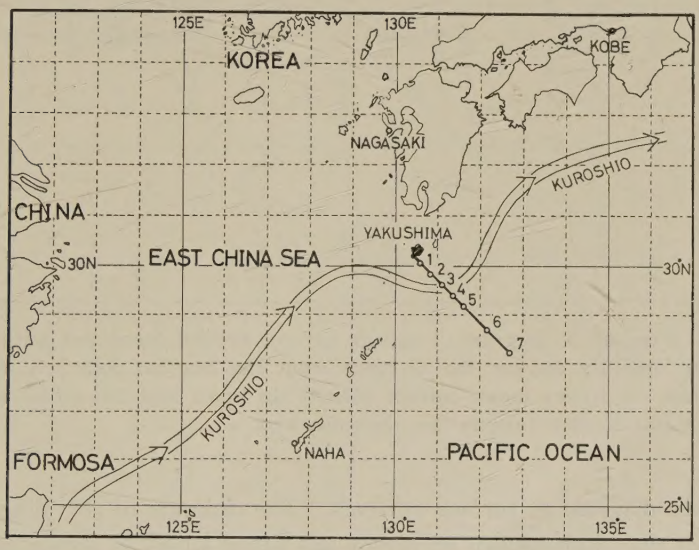

Fig. 1. Station location chart. The white circle shows hydrocast station and the dot denotes the original point of the section. The double line with arrows shows the schematic course of high-velocity zone of the Kuroshio.

the sea south of Japan, a fixed oceanographic section was set up in the sea southeast of Yakushima Island, south of Kyushu from May 1965 to February 1968. Observations were made on board the R/V *Chofu-maru*, Nagasaki Marine Observatory and the R/V *Shumpu-maru*, Kobe Marine Observatory. The section 160 nautical miles long consists of 7 hydrocast stations, which are spaced 20 nautical miles in the Kuroshio current and 40 nautical miles in the offshore half of the section (Fig. 1). In addition, 9 BT stations and 13 GEK stations were arranged on the section. These observations were planned to be carried out eight times a year to obtain a semi-annual and an annual variation. Unfortunately, however, the interval between successive observations was not uniform.

2. The fluctuation of surface currents

Surface currents were measured with GEK at intervals of 10 nautical miles in inshore half of the section and 20 nautical miles in the offshore half. Fig. 2 shows

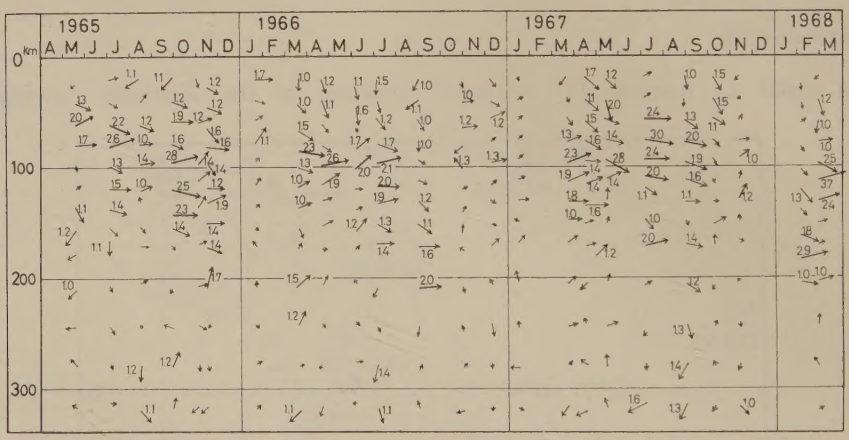

Fig. 2. Time-space diagram of surface current vectors measured with GEK. The ordinate denotes the distance from the original point. A numeral beside the arrows shows current velocity (in knot), and the arrow with no numeral denotes velocity less than one knot.

the time-space diagram of surface currents. The ordinate of this diagram denotes distance from the southwestern corner of the island which is shown with a dot in Fig. 1. The highest velocity in the Kuroshio is, on the average, found as distant as roughly 100 km from the coast, and the highest speed amounts to 3 knots or so

with nearly eastward direction. On the other hand, weak current is seen in the offshore region from 200 to 300 km, and at the end of the section southwestward currents are revealed frequently.

Time-space diagrams of the east and north components of surface velocity measured with GEK are shown in Figs. 3 and 4 respectively. Roughly speaking,

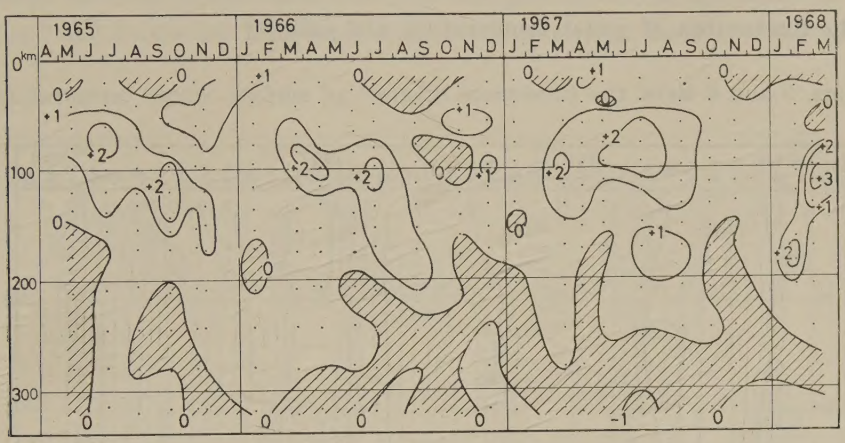

Fig. 3. Time-space diagram of east component of surface current (in knot) measured with GEK. Positive sign means eastward, and the negative area are shaded.

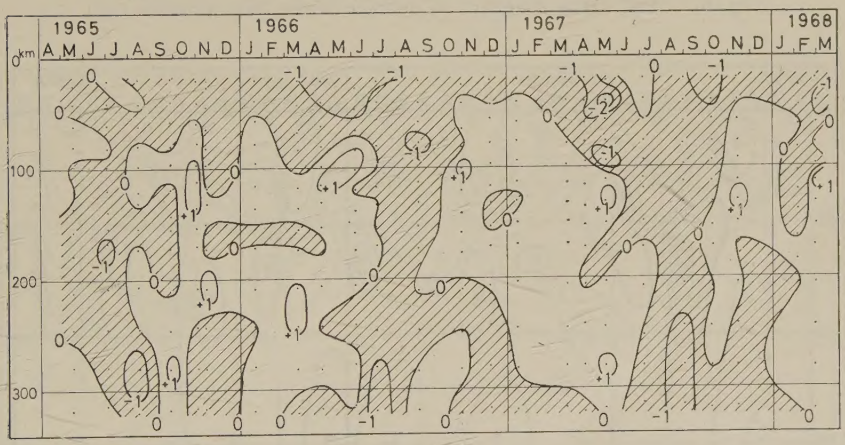

Fig. 4. Time-space diagram of north component of surface current (in knot) measured with GEK. Positive sign means northward, and the negative area are shaded.

the higher speed more than 2 knots in east component is found from spring to late summer, except in February 1968 when a cold water region extended further offshore. Though the north component is generally small and variable, southward components are seen in the entire section in summer. That is, the direction of the Kuroshio in summer is consistently southeastward or east-southeastward.

3. The fluctuation of water temperature and salinity

Figs. 5 and 6 show the time-space diagram of surface water temperature and

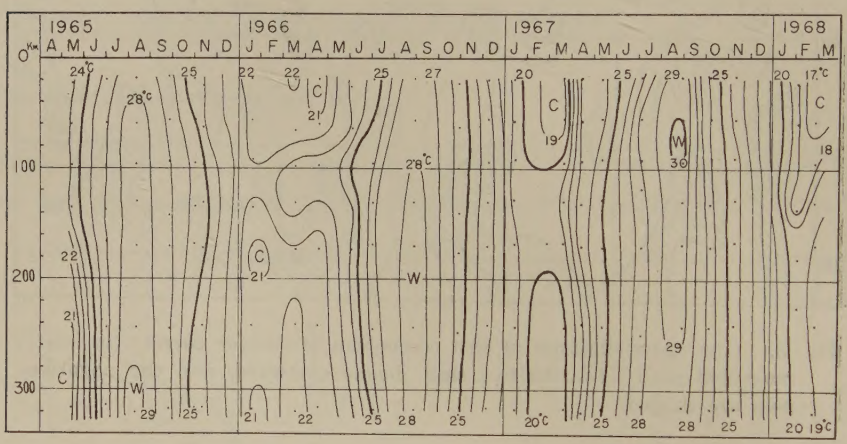

Fig. 5. Time-space diagram of surface water temperature (°C).

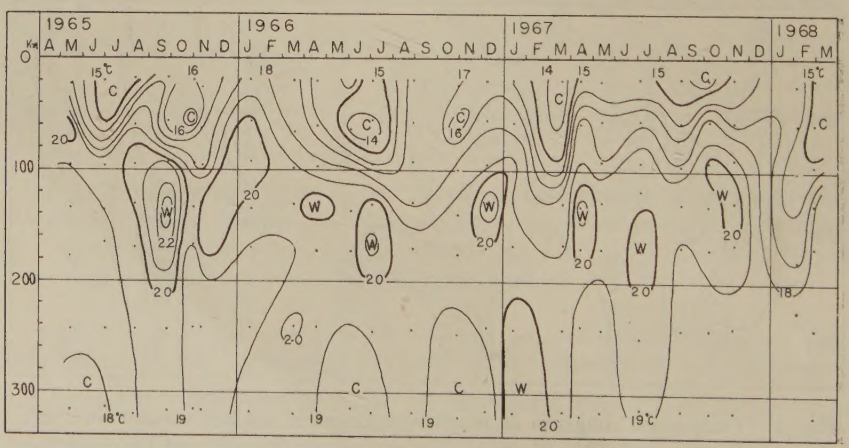

Fig. 6. Time-space diagram of water temperature (°C) at the depth of 200m.

temperature at a depth of 200m, respectively. As seen from these figures, the seasonal variation is outstanding at the sea surface, but it is hardly recognized at a depth of 200m. At the sea surface, maximum temperature occurs in summer and minimum appears in winter at all stations. From Fig. 6, a cold area is found in the coastal region northwest of the current-axis and the highest temperature appears in the zone of the warm core just southeast of the current-axis.

Figs. 7 and 8 show the time-space diagram of salinity at the sea surface and at

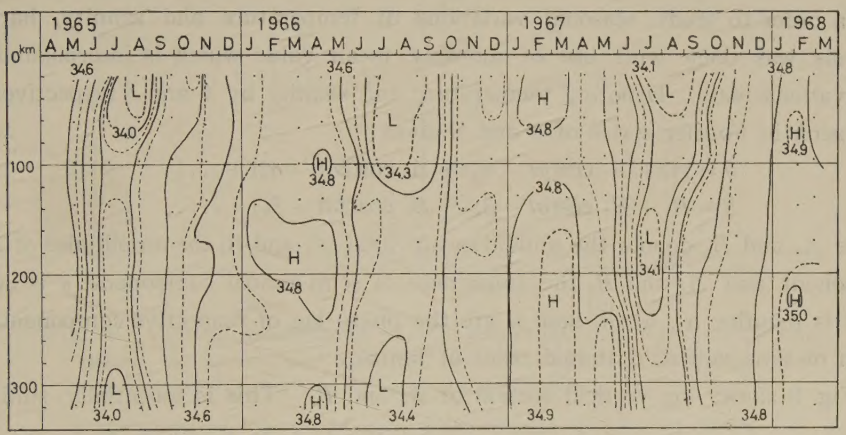

Fig. 7. Time-space diagram of surface salinity (‰).

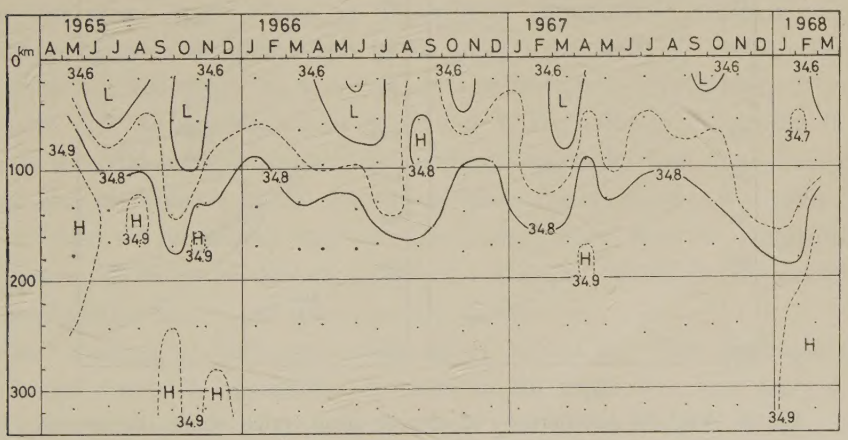

Fig. 8. Time-space diagram of salinity (‰) at the depth of 200m.

a depth of 200m respectively. The surface salinity is high in winter and low in summer, and decreases rapidly in May and June. This rapid decrease may be caused by great precipitation at the Baiu-front which exists stationarily near Japan from late May to early July. On the other hand, the seasonal variation of salinity can not be recognized at a depth of 200m (Fig. 8). At this layer, salinity is low in the coastal region and high in the offshore half of the section, and these areas are divided by the isohaline of nearly 34.8‰.

4. The results of harmonic analysis

In order to study seasonal variations of temperature and salinity, harmonic analysis was done with use of monthly mean value which is interpolated from observational data. Denoting temperature and salinity by θ and S respectively, the expansion in Fourier series of θ and S gives

$$\theta = A_0 + A_1 \cos(\sigma t - \alpha_1) + A_2 \cos(2\sigma t - \alpha_2) + \ldots.$$
$$S = B_0 + B_1 \cos(\sigma t - \beta_1) + B_2 \cos(2\sigma t - \beta_2) + \ldots.,$$

where A_0 and B_0 denote the annual mean value, A_1 and B_1 the amplitudes of annual component and A_2 and B_2 the amplitudes of semi-annual component; σ is 360°/12 and t is months; α_1, α_2, β_1 and β_2 are the phase lag of respective component. The origin of time is placed at mid point of January.

Fig. 9 shows the vertical section of A_0 and B_0. This is essentially similar to

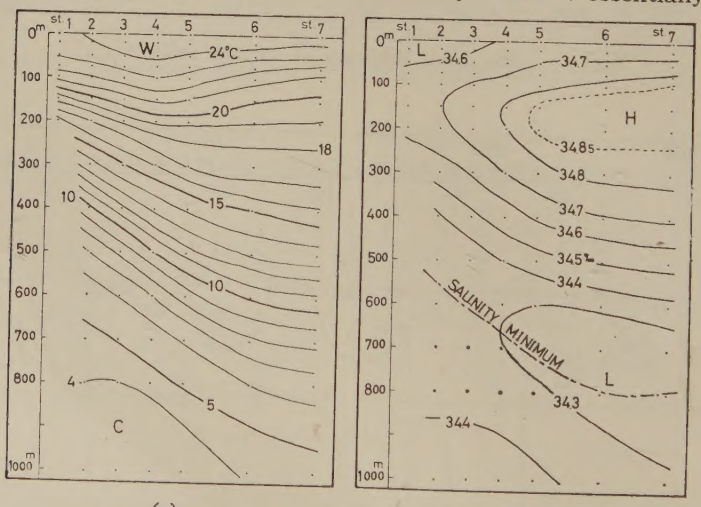

(a) (b)

Fig. 9. Vertical distributions of annual mean value along the section southeast of Yakushima Island. Left figure (a) is for temperature (A_0) in °C, and right (b) salinity (B_0) in ‰.

the section at each observation. It reveals warm core, main thermocline, Subtropical Mode Water, intermediate salinity minimum and so on.

Fig. 10 shows the vertical distribution of both A_1 and B_1. Both patterns in

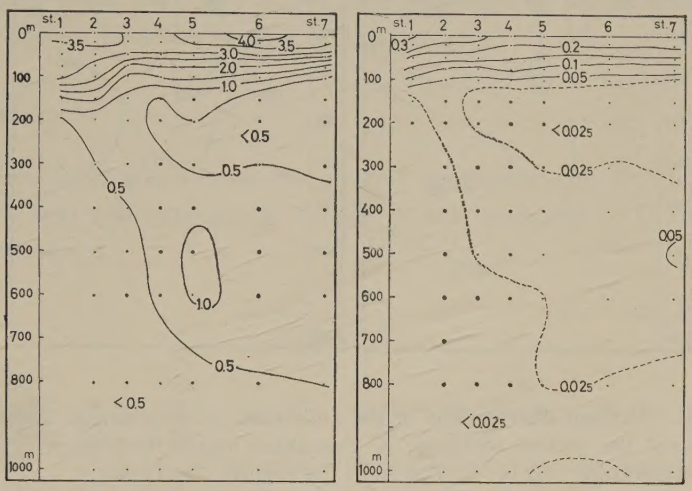

(a) (b)

Fig. 10. Vertical distributions of the amplitude of annual component along the section southeast of Yakushima Island. Left figure (a) is for temperature (A_1) in °C, and right (b) salinity (B_1) in ‰.

annual amplitude of temperature and of salinity are almost the same. In the upper 100 to 150m, the values of A_1 and B_1 are large and decrease rapidly with depth below this upper layer. That is, the annual variations of temperature and of salinity are extremly prominent only in the upper 100 to 150 m. On the other hand, the annual variations are so small in the deeper layer. Especially, it may be noticeable that the smallest values of A_1 and B_1 are found in the depths of 100 to 300m at the offshore area south of the current-axis of the Kuroshio. This characteristic part corresponds to the Subtropical Mode Water (MASUZAWA, 1969). Therefore, it may be considered that the Subtropical Mode Water is maintained at a nearly constant state throughout a year, and is hardly fluctuated by heating, cooling, precipitation and evaporation near the surface.

Fig. 11 shows the vertical distributions of A_2 and B_2. The amplitude (B_2) in semi-annual variation of salinity is large in the upper 50m, and decreases with depth below this surface layer. In this figure the sudden drop of salinity in June may be due to excessive precipitation, and the vertical uniformity of it from late

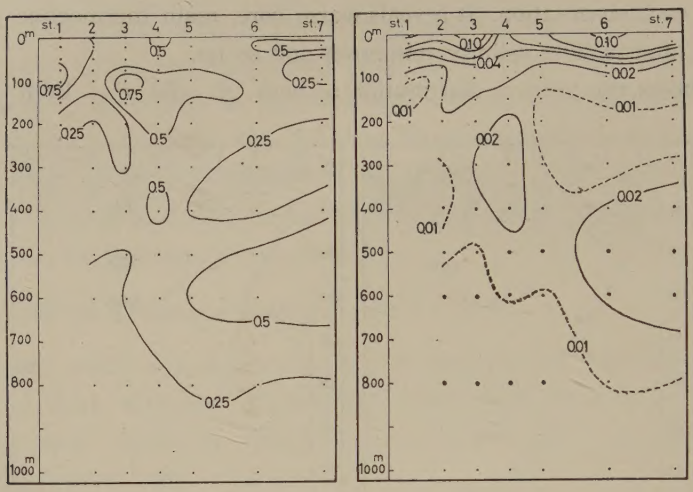

(a) (b)

Fig. 11. Vertical distributions of the amplitude of semi-annual component along the section southeast of Yakushima Island. Left figure (a) is for temperature (A_2) in °C, and right (b) salinity (B_2) in ‰.

fall to early spring due to excess of evaporation over precipitation. Comparatively large amplitude (A_2) in semi-annual variation of temperature is seen just south of the current-axis in the depths of 100 to 200m.

The phase lags α_1 and β_1 of annual variation of temperature and salinity are shown in Fig. 12. The phase lag approximately determines the time for the occur-

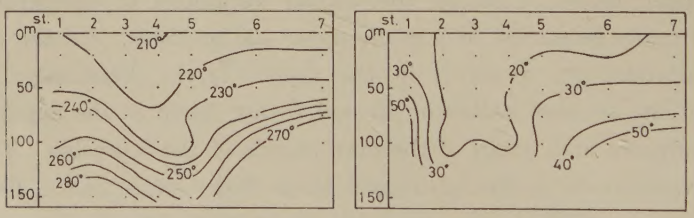

(a) (b)

Fig. 12. Vertical distributions of the phase lag of annual component along the section southeast of Yakushima Island. Left figure (a) is for temperature (α_1) in degree, and right (b) salinity (β_1) in degree.

rence of the maximum or the minimum. Roughly speaking, the values of α_1 and β_1 are relatively small at the vicinity of the current-axis, and increase with depth

in nearly all regions. Seeing these distributions in detail, the rate of increase with depth of α_1 is greater than that of β_1, and the value of α_1 is small at the warm core just southeast of the current-axis. The difference between α_1 and β_1 at the surface layer is about 200°, that is, the time of maximum temperature nearly corresponds to one of minimum salinity at this layer.

Acknowledgement

The author wishes to express his greatest appreciation to Dr. J. MASUZAWA for his kind help and suggestions throughout this work and to Dr. S. MORIYASU for his useful advice.

References

FUKUOKA, J. and I. TSUIKI (1954): On the variation of chlorinity in the Kuroshio Area. *Oceanogr. Mag.*, **6**(1), 15–23.

ICHIE, T. (1956): On the annual variation of chlorinities at the upper layer of the Kuroshio. *Oceanogr. Mag.*, **7**(2), 87–93.

KOIZUMI, M. (1955): Researches on the variations of oceanographic conditions in the region of the ocean weather station "Extra" in the North Pacific Ocean. *Pap. Met. Geophys.*, **6** (2), 185–201.

MASUZAWA, J. (1954): On the Kuroshio south off Shiono Misaki of Japan. *Oceanogr. Mag.*, **6**(1), 25–33.

MASUZAWA, J. (1969): Subtropical Mode Water. *Deep-Sea Res.*, **16**, 463–472.

MORIYASU, S. (1969): On the change of monthly sea surface temperature in the Western North Pacific (I). *Oceanogr. Mag.*, **21**(1), 1–11.

WYRTKI, K. (1965): The annual and semiannual variation of sea surface temperature in the North Pacific Ocean. *Limnol. Oceanogr.*, **10**(3), 307–313.

屋久島南東における黒潮の季節変動について

土　田　武　雄

（長崎海洋気象台）

黒潮国際共同調査（CSK）の一環として，九州南方の屋久島南東沖における黒潮の季節変動を調査するため，1965年5月から1968年2月にわたって合計24回（年間8回）の定線海洋観測が長崎海洋気象台の長風丸と神戸海洋気象台の春風丸によって実施された．観測線はその全長が160海里で黒潮を横切るように設定され，またこの線上に配置された観測点の数は各層7点，BT 9点およびGEK 13点である．

表面海流は平均的にみて屋久島沿岸から100 km付近に最強部があってほぼ東向きの流れを示し，またその沖合では流速が次第に小さくなり，さらに距岸 300km 付近ではときどき南西向きの流れがみられる．季節的な特徴としては，おおむね春から初秋までの期間において，主流域の流速が大きくなり逆に冬季において比較的小さな流速を示すことがあげられる．

観測された水温および塩分の資料に基ずいて調和分解をおこない，その調和定数の鉛直断面図を作成した．これらの図によれば，水温および塩分の両者とも年変化の振幅は概略的にみて表面から100 ないし 150m 層まではかなり大きくまた深さとともに次第に小さくなる傾向を示しているが，150m層以深では全般に小さく，特に亜熱帯モード水に相当する150ないし 300m 層付近ではきわめて小さいことが注目される．

The Oceanographical Magazine
Vol 23, No. 1, pp. 11 to 19, December 1971

On the change of monthly sea surface temperature in the Western North Pacific (III)

Shigeo MORIYASU

Meteorological Research Institute

(Received August 31, 1971)

Abstract: A model is applied to time change of the ten-day mean sea surface temperature at the ocean weather station, Tango, to the south of Japan as an initial step to prediction of the monthly mean sea surface temperature. In this model, time change of the sea surface temperature is dependent on the sea surface temperature and amount of heat exchange between the sea and the atmosphere, and other factors take normal values. Since the results are fairly satisfactory, estimation of the ten-day mean sea surface temperature is tried by integrating equation of its time change numerically. The bulk method is used to obtain amount of heat exchange between the sea and the atmosphere. Of required meteorological elements, air temperature and vapour pressure are approximated by a linear function of sea surface temperature. Error caused by this approximation is not important for practical purposes. Then, wind speed and cloudiness are necessary, but they are not predicted. Here, their normal values are used as an instrument. Probable error is 0.5°C or so and this simplified method is useful for prediction if errors of this magnitude are accepted. Furthermore, the ten-day mean sea surface temperature is evaluated for various initial values under special conditions.

1. Introduction

The author discussed the change of monthly sea surface temperature in relation to the amount of heat exchange between the sea and the atmosphere (MORIYASU, 1969, 1970). And, it was inferred that the variation of sea surface temperature depends roughly on the amount of heat exchange between the sea and the atmosphere for the sea north of 20°N in the Western North Pacific.

In this paper, it is discussed how the relation derived in the previous paper is applied to the ten-day mean sea surface temperature at the ocean weather station, Tango (29°N, 135°E), and a trial is made as an initial step to prediction of the monthly mean sea surface temperature, though the model is much simplified. The observations at the ocean weather station are made very accurately. It is why data at Tango are used to test the applicability of the model.

2. The variation of temperature in the surface layer

The model used in this paper is the one which is derived in the previous paper (MORIYASU, 1970). According to the model, variation of the sea surface temperature is given by the equation,

$$\frac{d\theta_0}{dt} = a\theta_0 + bQ_{SA} + c\,,$$

$$a = k/D, \quad b = 1/(\alpha D c_p)\,,$$

$$c = -k\theta_D/(\alpha D) + Q_H/\alpha,\ Q_H = -\vec{V}\cdot grad\bar{\theta} + K_H\nabla^2\bar{\theta}\,,$$

where

Q_{SA} : the amount of heat exchange between the sea and the atmosphere,
D : thickness of the surface layer,
c_p : specific heat of sea water,
θ_D : water temperature at the bottom of the surface layer,
$\bar{\theta}$: mean water temperature in the surface layer,
$\vec{V}$: mean horizontal velocity in the surface layer,
K_H : horizontal eddy diffusion coefficient for heat.

α is a constant which is given by an assumption, $\bar{\theta} = \alpha\theta_0$. k is expressed by $k = w_D - k'$, where w_D is the downward speed at the bottom of the surface layer ($z = D$) and k' is a constant introduced in an assumption that heat exchange at the bottom of the surface layer is proportional to $\bar{\theta} - \theta_D$. a, b and c express the effects of advection and mixing and fluctuate with time. If these effects are assumed to be constant, a, b and c are also taken as constant. Then, the variation of sea surface temperature is dependent on the sea surface temperature and the amount of heat exchange between the sea and the atmosphere, Q_{SA}, which is obtained as a function of sea surface temperature, air temperature, vapour pressure, cloudiness and wind speed by the bulk method. Therefore, on such assumptions, the variation of the sea surface temperature can be estimated when a, b and c are known and these elements are given.

3. Application to the ten-day mean sea surface temperature at Tango

Ocean weather station "Tango "located at 29°N, 135°E is occupied by an ocean weather ship from June to October every year and ten-day mean values of meteorological elements are compiled in the Geophysical Review published by the Japan Meteorological Agency. In this paper, the data from 1952 to 1966 are used.

Here, Q_{SA} is computed by the bulk method which is used in the previous paper (MORIYASU, 1969), and centered difference is substituted for $d\theta_0/dt$. This procedure is executed for the second ten-day of June (the 17th ten-day) to the first ten-day of October (the 28th ten-day). For each ten-day, 13—15 sets of samples are given and the value of three parameters, a, b and c, are obtained by the method of least squares. Probable error of the relation is less than 0.3°C/10 days and the approximation is satisfactory for practical purposes. Thus, the model in the previous section is inferred to be applicable to this case. The error is considered to be brought about by neglecting the year-to-year variation of advection and mixing.

Now, the sea surface temperature in a ten-day is estimated from the sea surface temperature in the preceding ten-day by integrating the relation given in the previous section. As Q_{SA} is a function of sea surface temperature, air temperature, vapour pressure, wind speed and cloudiness, four elements except for sea surface temperature are necessary to execute numerical integration if they are assumed to be independent of the sea surface temperature. Observed values are given to these elements and Runge-Kutta-Gill's method is taken. Then, the root mean square (RMS) of deviations from observed temperature is less than 0.7°C. This is called Case A (Fig. 1). The computation is made as a preliminary step to extrapolation

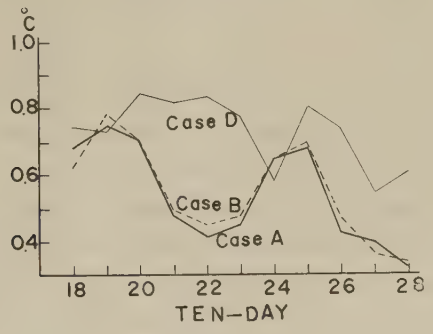

Eig. 1. Root mean squares of deviation of computed value from observed one.

of sea surface temperature which will be described in Section 5.

4. The simplification of the model

In Case A, four meteorological elements are necessary to compute Q_{SA} by

using the bulk method. These elements are expected to be related to sea water temperature. If the relation is known, the number of parameters can be reduced. Explicit relations, however, have not been obtained yet. Air temperature is expected to be closely related to sea surface temperature. Correlation coefficients between the air temperature and the sea surface temperature are greater than 0.8 except for the second ten-day of October. The coefficient for this ten-day is 0.718. As high correlation is found between the air temperature and the sea surface temperature, it is admitted to approximate the air temperature as a linear function of the sea surface temperature. Probable error is less than 0.3°C for most ten-days (Table 1). Vapour pressure is not correlated with the sea surface temperature.

Table. 1. Probable errors of air temperature in °C (T_a), vapour pressure of air in mb (E_a), sensible heat in 10^{-3} ly/min (Q_c) and latent heat in 10^{-3} ly/min (Q_e).

Ten-day	16	17	18	19	20	21	22	23	24	25	26	27	28	29
T_a	0.20	0.27	0.21	0.15	0.20	0.16	0.17	0.12	0.12	0.11	0.16	0.22	0.23	0.39
E_a	1.10	0.17	0.82	0.78	0.90	0.59	0.49	0.48	1.62	0.91	0.67	1.06	1.66	1.44
Q_c	3.7	5.1	3.5	2.6	3.1	2.7	3.2	2.4	2.1	1.9	2.6	4.5	6.8	8.9
Q_e	30.5	20.3	21.2	20.5	21.1	15.4	13.6	14.9	42.6	24.0	16.3	32.6	51.9	50.0

Though it is not rational to take vapour pressure as a function of the sea surface temperature, it is expressed as a linear function of the sea surface temperature with probable error less than 1.5mb for most ten-days (Table 1).

The process is not based on theoretical considerations, but is taken for convenience's sake to reduce the number of parameters, even though it is supposed that the error of Q_{SA} is made larger by the simplification. According to the bulk method, Q_b and Q_c are dependent on temperature and vapour pressure, so that the accuracy is influenced by the above simplification, but their magnitude is not large. Thus, error of these two elements is not important. Q_e is much larger in the magnitude than these two elements and the error controls error of Q_{SA}. Error of Q_e caused by the simplification is shown in Table 1 and is about 15% of the amount of Q_e on an average.

If the simplification mentioned above is taken, estimation of the sea surface temperature is possible when wind speed and cloudiness are known. Now, these two elements are given and numerical integration is executed as in Case A in the

previous section. This is called Case B. RMS of deviations from observed temperature is slightly larger than RMS for Case A (Fig. 1). Therefore, the simplification is useful for practical purposes. From the results of the experiments, the sea surface temperature in the following ten-day is predicted with the accuracy noted above if wind speed and cloudiness are predicted with sufficient accuracy.

5. Results under specified conditions

In the previous two sections, the subject is the estimation of the sea surface temperature in the following ten-day and the accuracy is estimated. If the sea surface temperature in a ten-day is given as the initial value and the procedure is repeated, the sea surface temperature is estimated in order for arbitrary ten-day. Here, values of a, b and c are specified for each ten-day. The simplification introduced in Section 4 is taken in this trial and wind speed and cloudiness should be given for each ten-day. Even if observed values are given to these elements, it is inferred that the error is larger than the error for Cases A and B in general. Because, accumulation of the errors is caused by repetition of computation.

Computations are made for three cases. The second ten-day of June (the 17th ten-day) is taken as the initial ten-day and the sea surface temperature is estimated for the third ten-day of June (the 18th ten-day) through the first ten-day of October (the 28th ten-day) (Fig. 2). Three cases are dependent on the choice of wind speed and cloudiness for each ten-day. The first case, Case C, is for the minimum value from 1952 to 1966. The second case, Case D, is for the mean value in the period. The third case, Case E, is for the maximum value in the period.

In Case C (Case E), Q_{SA} in each ten-day is nearly maximum (minimum) for a given sea surface temperature since Q_S is maximum (minimum) and Q_b, Q_c and Q_e are minimum (maximum). Cases C and E are not actual ones, but assumed ones in which wind speed and cloudiness keep extreme values from the second ten-day of June (the 17th ten-day) to the first ten-day of October (the 28th ten-day). And, observed value of the sea surface temperature is expected to be between computed values for the two cases.

Case D is also an assumed case in which wind speed and cloudiness keep normal values, and such a case is not expected to appear actually though it is not an extreme case. RMS of deviations from observed value is less than 0.84°C (Fig. 1). If error of such a magnitude (probable error less than 0.57°C) is permitted for prediction of the sea surface temperature, estimated value for this case is taken as

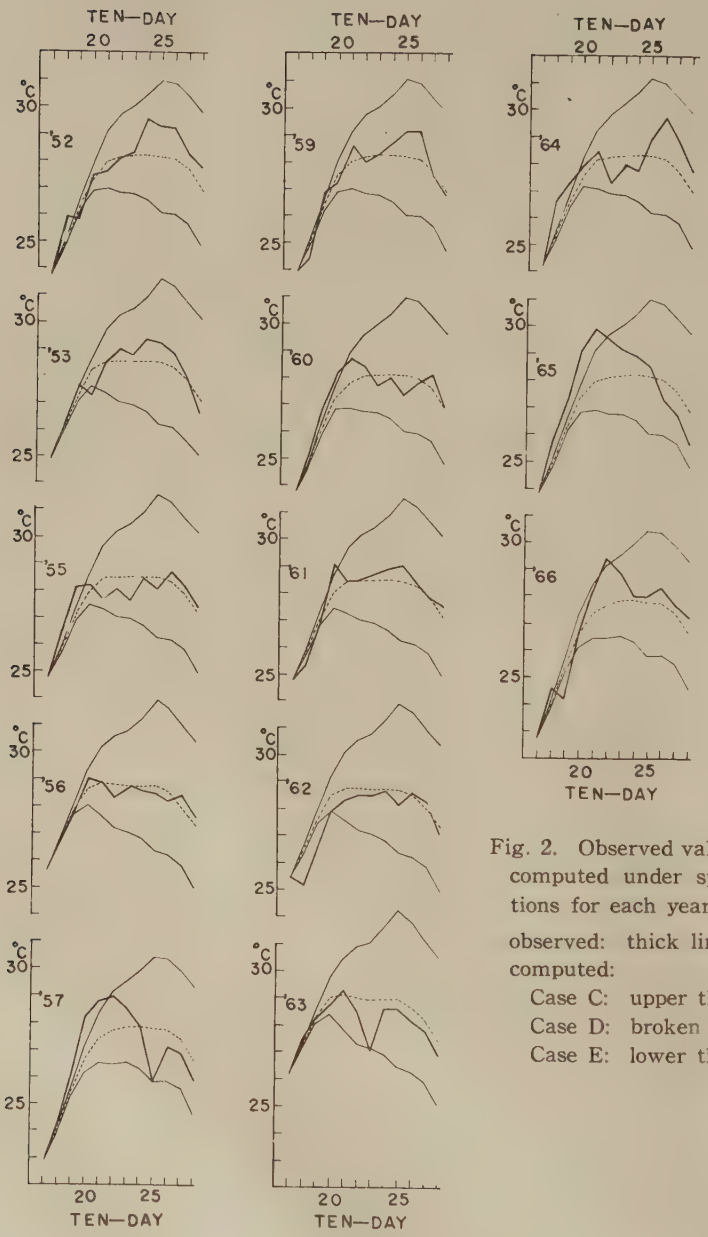

Fig. 2. Observed value and values computed under specified conditions for each year.

observed: thick line
computed:
Case C: upper thin line
Case D: broken line
Case E: lower thin line

predicted value. In other words, the sea surface temperature is predicted with probable errors less than 0.57°C if normal values are given to wind speed and cloudiness.

According to our model, the sea surface temperature is dependent on the initial sea surface temperature, wind speed and cloudiness. Fig. 3 shows the change of

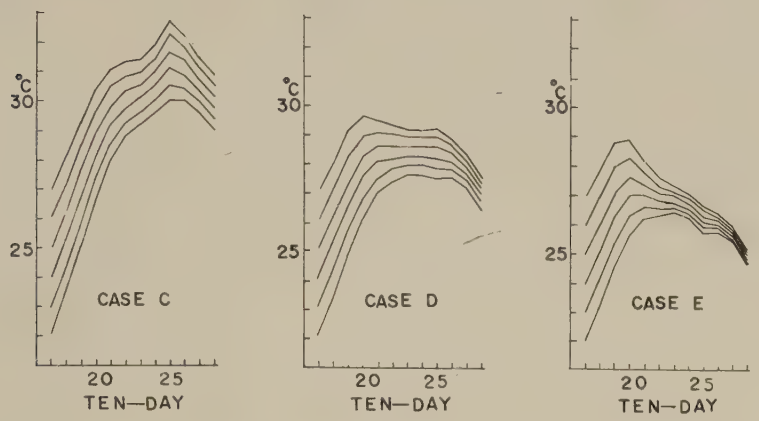

Fig. 3. Computed values for various nitial values under specified conditions.

estimated sea surface temperature at Tango with initial value for Cases C, D and E. The influence of initial value on estimated value is smaller in Case E than in Case C. The difference of 5°C in the initial value produces the difference of about 2°C for Case C and of about 0.5°C for Case E in estimated value for the first ten-day of October (the 28th ten-day). The difference of estimated value for the first ten-day of October (the 28th ten-day) due to the cases is about 6°C and about 4.5°C for the initial value of 27°C and 22°C, respectively. This means that wind speed and cloudiness play an important role in determining the sea surface temperature at Tango. The difference in the initial value is not so effective for the difference of estimated value.

6. Discussion and concluding remarks

The model used in this paper is constructed on the assumption that effects of advection and mixing for each ten-day do not change with year. The effect should be estimated theoretically, but we have no reliable data of elements necessary to

determine them. This is why normal conditions are assumed. JACOB (1967) and ADEM (1970) estimated these effects theoretically, but many assumptions were made and high accuracy is not expected in the estimation.

It is shown in Section 3 that the model is applicable to the variation of the ten-day mean sea surface temperature at Tango. Satisfactory results are due to the condition that the ocean weather station is located in a region of fixed water mass and that another water mass never occupies the station. It is doubtful to apply the model to station near the coast or polar front. Error is expected to be reduced if these effects are estimated with sufficient accuracy.

According to the model, the sea surface temperature is determined by amount of heat exchange between the sea and the atmosphere. Thus, for estimation of the sea surface temperature, some elements are necessary. Conversely speaking, when the elements are predicted, prediction of the sea surface temperature is possible. In the simplified model, extended prediction of wind speed and cloudiness are required. At present, it is impossible than to be difficult. Then, their normal values are used as an expedient means. These elements are input independent of the sea surface temperature in this model, but, essentially, they should be also taken as the object of prediction, that is, these elements are to be predicted together with the sea surface temperature in a combined system which consists of atmosphere and hydrosphere.

Air temperature and vapour pressure are expressed as a linear function of the sea surface temperature. Since air temperature is closely correlated with the sea surface temperature as mentioned in Section 4, it is reasonable to apply the relation to air temperature. Here, it is not discussed what relation is most appropriate. On the other hand, there is no basis to take the vapour pressure as a linear function of the sea surface temperature. Neither the correlation is close, nor simple theoretical relation is expected. Thus, this process is taken only for convenience's sake. Though increase in RMS of deviations caused by the simplification is slight, some improvements are to be made on this point.

A series of the study are on the monthly mean sea surface temperature, though the ten-day mean sea surface temperature is the subject of this paper. It is inferred that the model is applicable to the ten-day mean sea surface temperature. And, the next step is to discuss if the procedure is applicable to the monthly mean sea surface temperature.

Acknowledgements

The author wishes to express his gratitude to Dr. T. NAN'NITI for his valuable advices and to Miss K. OKADA of Meteorogical Research Institute for her help in the study.

References

ADEM, J. (1970): On the prediction of mean monthly ocean temperatures. *Tellus*, **22** (4), 410–430.

JACOB, W. J. (1967): Numerical semiprediction of monthly mean sea surface temperature. *Journ. Geophys. Res.*, **72** (6), 1681–1689.

MORIYASU, S. (1969): On the change of monthly sea surface temperature in the Western North Pacific (I). *Oceanogr. Mag.*, **21** (1), 1–11.

MORIYASU, S. (1970): On the change of monthly sea surface temperature in the Western North Pacific (II). *Oceanogr. Mag.*, **22** (1), 27–36.

北西太平洋の月平均海面水温の変化について (III)

森　安　茂　雄

(気象研究所)

この報告における旬平均海面水温についての試みは月平均海面水温の予測への一つの段階として行なったものである．本州南海の南方定点の旬平均海面水温の変動に，ある簡単なモデルを応用した．このモデルでは旬平均海面水温の変動は海面水温と海洋・大気間の熱交換量とに関係するとし，影響を与えるほかの要素は平年値をとるとしている．応用した結果はかなり満足すべきものであった．従ってその変動を示す式を数値積分して旬平均海面水温の推算を試みた．海洋・大気間の熱交換量はバルク法によって求めたが，必要な気象要素の中，気温と空気の蒸気圧を海面水温の一次式で近似した．この近似によって生ずる誤差は実際的にはそれ程大きなものではない．このようにすれば，残る要素は風速と雲量であるが，これらを予測することはできない．そこで，これらの値として平年値を使った結果，次の旬の平均海面水温予測の確率誤差は0.5°C前後となり，もしこの程度の誤差が海面水温の予測に許されるならば，この簡単化した方法を予測に使うことができるのであろう．また，初期値と風速，雲量に種々の値を与えて旬平均海面水温の推算を行ない，初期値と途中の条件とが与える効果についても調べた．

The Oceanographical Magazine
Vol. 23, No. 1, pp. 21 to 32, December 1971

Distribution of chlorophyll and phaeophytin in the Sea of Japan

by

Mamoru OHWADA

Maizuru Marine Observatory

(Received September 30, 1971)

Abstract: Fluorometric determination of chlorophyll-a and phaeopigments in the Sea of Japan was carried out in October 1969.

Maximum concentration of chlorophyll pigments was determined to be at or just below the seasonal pycnocline, namely from 20 to 75m depth. The depth of the chlorophyll maximum layer coincided well with that of the maximum layer of the oxygen supersaturation.

Population density of living phytoplankton was not always correlated with the concentration of chlorophyll pigments. The first reason may be that the phytoplankton community is composed of different-sized individuals containing different volumes of chlorophyll, and the second, the adaptation of phytoplankton to dim light.

1. Introduction

In the seas adjacent to Japan, studies on phytoplankton pigments in the Sea of Japan (KOBLENTZ-MISCHKE, 1960) are quite rarer than those in the Pacific (ARUGA and ICHIMURA, 1968; ICHIMURA and SAIJO, 1959; ICHIMURA, SAIJO and ARUGA, 1962; KAWARADA and SANO, 1969; Saijo, IIZUKA and ASAOKA, 1969).

The purpose of this study is to clarify the general distribution pattern of chlorophyll pigments and to find out its relation to other environmental factors. Using the fluorometric technique (YENTSCH and MENZEL, 1963; SAIJO and NISHIZAWA, 1969), determinations of chlorophyll pigments were carried out on board the R.V. *Ryofu Maru* and *Seifu Maru* at thirty stations in the Sea of Japan in October 1969 (Fig. 1). The oceanographical investigations in the Sea of Japan were made by the five vessels of the Japan Meteorological Agency (OHWADA and TANIOKA, 1971).

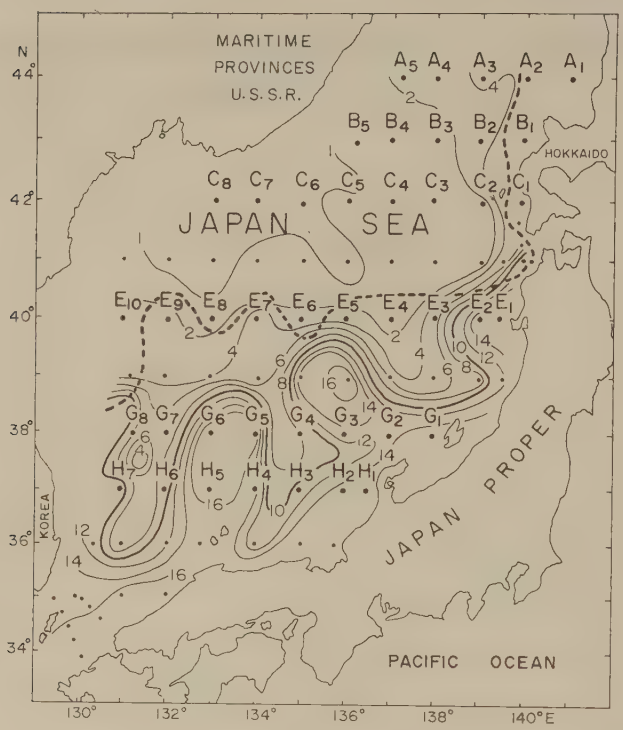

Fig. 1. Location of sampling stations and water temperature at 100 m depth. The cold water at the northwestern part of the broken line contains supersaturated dissolved oxygen showing 115–130% at 30–50m depths.

2. Materials and methods

Water samples of 250m*l* for determination of chlorophyll and phaeophytin were collected from depths of 10, 20, 30, 50, 75, 100, 150, 200, 300, 400, 500m with Nansen bottles, at the stations on A, B, C, G, and H line. Surface water samples of the same volume were dipped by a bucket.

Treatment of samples and calculation method of chlorophyll pigments are the same as those stated by KAWARADA and SANO (1969). Before filtration 5mg of magnesium carbonate was added to 250m*l* of water sample and then the sample water was filtered through a glass fiber filter of 24mm in diameter (Reeve Angle 984 H Ultra Filter). When the measurements could not be made immediately after filtration, the filter was put in a desiccator and stored in a refrigerator for several days.

The filter was ground by a pestle in a mortar with 2 or 3m*l* of 90% acetone. The contents of the mortar were carefully washed with 5 or 6m*l* of 90% acetone into a centrifuge tube with a cap and centrifuged at 3000 rpm for 5 minutes. The supernatant was carefully decanted into a fluorescence cuvette and made up to 10.0m*l* with 90% acetone.

The emission of the acetone extract was determined by a Hitachi model FPL-2 fluorometer which was previously adjusted by the standard solution. For preparing the standard solution, 1 mg of fluorescein sodium salt was dissolved in one liter of distilled water. After this process two drops of 0.5 N HCl were added directly to the extract in the cuvette which was then shaken for 15–20 seconds for the conversion of chlorophyll to phaeophytin. After 3 minutes the fluorescence was read again.

The concentrations of chlorophyll and phaeophytin were calculated by the following equations:

$$\text{Chlorophyll-a} \quad (\mu g/l) = 1.27\,(F_o - F_a)\frac{v}{V} \cdot \frac{1}{10}$$

$$\text{Phaeophytin-a} \quad (\mu g/l) = 1.27\,(4.7F_a - F_o)\frac{v}{V} \cdot \frac{1}{10}$$

where: F_o=fluorescence before acidification,
F_a=fluorescence after acidification,
V =volume of sample (m*l*),
v =volume of acetone extract (m*l*).

In order to compare the vertical distributions of chlorophyll-a and phaeopigments with the vertical distributions of phytoplankton, 250 to 500 m*l* of sample waters for the phytoplankton study were taken from the same Nansen bottles together with the sample waters for the measurement of pigments, at the stations of the B, C, and E line. Phytoplankton were counted under the microscope distinguishing between living cells and dead ones, and the results have been already reported by OHWADA (1971).

3. Results and discussion

(1) *Maximum layer of pigments*

The vertical distributions of chlorophyll-a and phaeophytin-a in the Sea of Japan are characterized by the maxima which occur in the upper 75 m (Fig. 2 a, b, and

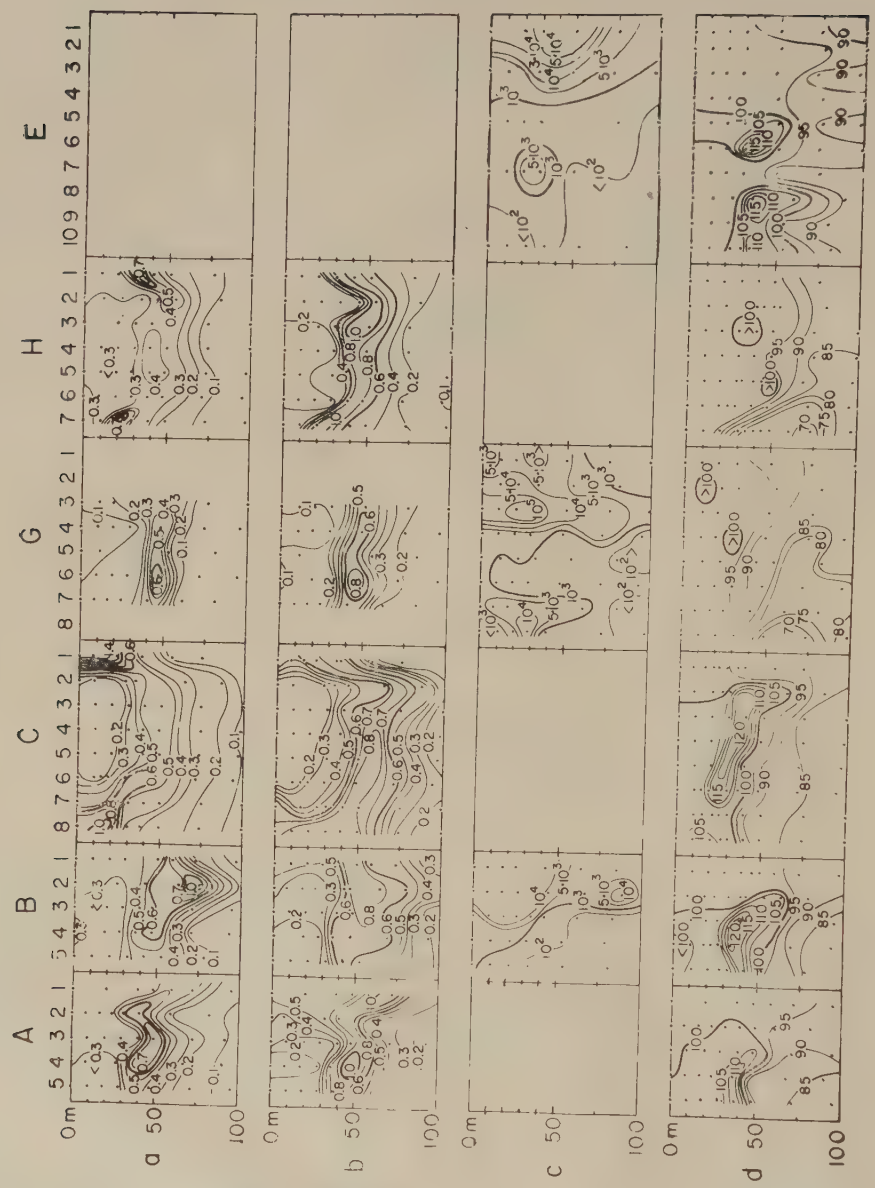

Fig. 2. Vertical distribution of pigments (μg l), number of diatoms (cells l), saturation percentage of dissolved oxygen, temperature (°C), salinity (‰), stability (10^6 E), and phosphate-phosphorus (μg-atoms l). a: chlorophyll-a, b: phaeophytin,

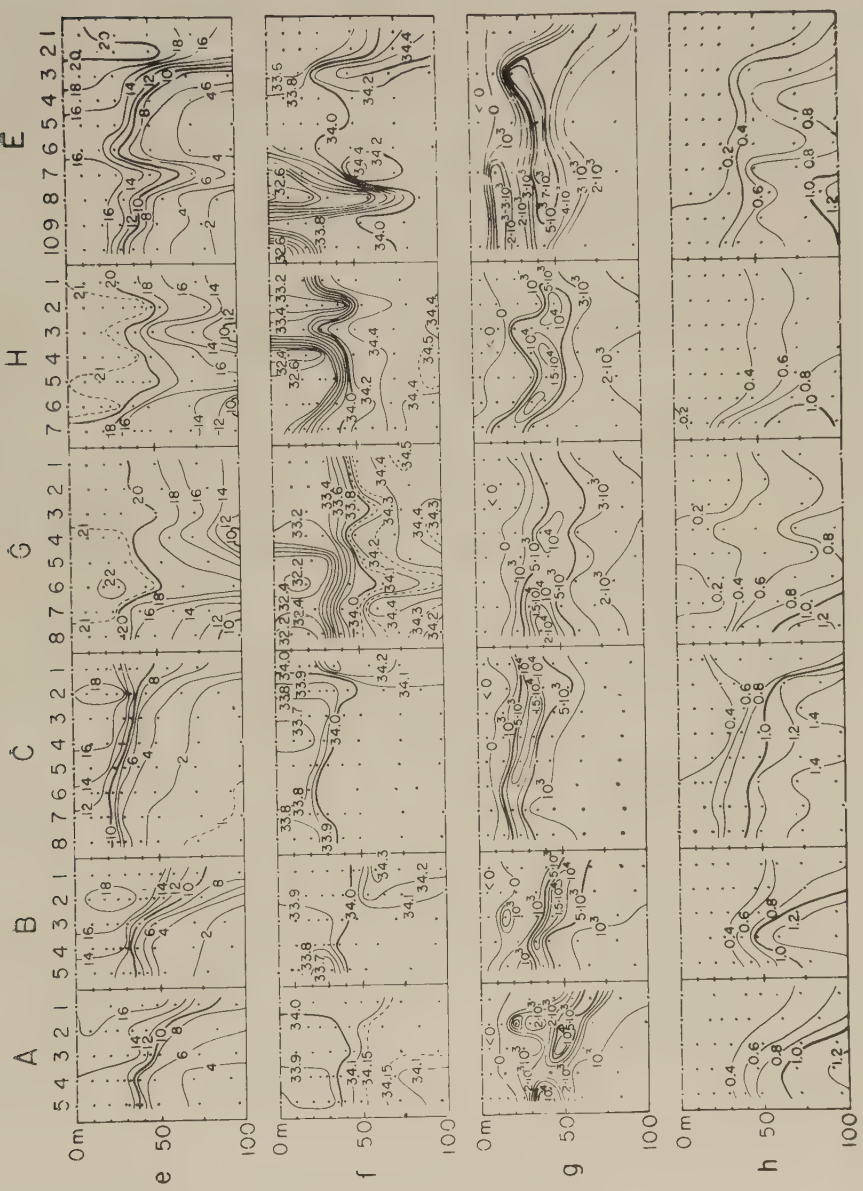

c: number of living diatoms, d: saturation percentage of oxygen, e: temperature, f: salinity, g: stability, h: phosphate-phosphorus.

Fig. 3). In the levels below 100 m, the concentration of chlorophyll-a decreases to less than 0.1 $\mu g/l$ and that of phaeophytin-a diminishes to less than 0.2 $\mu g/l$.

At the stations of the H line in the Tsushima Warm Current, the chlorophyll-a maximum is found at depths ranging from 20 to 50 m, and the depth of the phaeopigments maximum coincides with that of chlorophyll-a maximum. The percentage of chlorophyll-a to the total of chlorophyll-a and phaeophytin-a is generally 40 to 60% in the upper 50 m, decreasing to 30% at the bottom of the euphotic zone (about 80 m) which is estimated from the Secchi disk reading, and to about 20% at the depth of 100 m. At St. H_1 near the coast of Japan Proper, the maxima of chlorophyll-a and phaeophytin-a are at the depth of 30 m, showing 0.7 $\mu g/l$ and 1.0 $\mu g/l$, respectively. At St. H_7 near the coast of East Korea, the maxima of both pigments are at the depth of 20 m, and the values are nearly the same as those at St. H_1. The maxima of the pigments at the stations between the two stations mentioned above are found at 40–50 m, and the values are 0.4–0.5 $\mu g/l$ (chlorophyll-a) and 0.8–1.0 $\mu g/l$ (phaeophytin-a). At the stations of the G line, though coastal data are lacking, the maxima of the pigments are in the depths of 40 to 50 m, and the values are 0.4–0.6 $\mu g/l$ and 0.6–0.8 $\mu g/l$, respectively.

On the C line, as on the H line, concentration maximum of chlorophyll-a is found at both coastal stations. Especially at St. C_1 near the west coast of Hokkaido, contents of chlorophyll-a are more than 1.4 $\mu g/l$ at 15m, whereas the concentration of phaeophytin-a is not so large, being 0.6 $\mu g/l$ at the same depth. It is reasonably thought that the phytoplankton at this depth are actively doing photosynthesis, because the phytoplankton population is the largest in this survey, reaching 10^6 cells/l and the percentage of chlorophyll-a to the total pigments is more than 74%. At St. C_8 near the coast of Maritime Provinces of U.S.S.R., the maxima of the pigments are found at the depth of 20m, being 1.05 $\mu g/l$ of chlorophyll-a and 0.95 $\mu g/l$ of phaeophytin-a. But the photosynthesis there must be not so active, since the percentage of chlorophyll-a to the total pigments is only 55%. Chlorophyll-a maximum (0.5–0.6 $\mu g/l$) at the stations between these two stations is found in the depths of 30 to 50m, while phaeophytin maximum (0.6–0.8 $\mu g/l$) lies in the depths of 40 to 70m.

At St. B_2 in the northward flowing branch of the Tsushima Warm Current (Fig. 2, e,f), chlorophyll-a maximum of 1.4 $\mu g/l$ is found at the depth of 75m where the second maximum of living diatom population exists (Fig. 2c). At the other stations of the B line chlorophyll-a maxima are found in shallower depths (50–60m), being 0.6–0.7 $\mu g/l$. Phaeophytin-a maxima at the stations of the B line are found

at 50m, being 0.6-0.8$\mu g/l$.

At St. A_1 in the northward flowing branch of the Tsushima Warm Current, the maxima of chlorophyll-a and phaeophytin-a are found at 60m and 70m, respectively, while at the other stations of the A line in the cold waters both of the maxima lie in shallower depths (40–50m).

(2) *Chlorophyll-a maximum layer and vertical stability of water*

As mentioned above, the subsurface maximum layer of chlorophyll-a in the Sea of Japan in autumn exists in the upper 75m. These distributional patterns of the pigments are closely related to the hydrographical conditions. The depth of the chlorophyll-a maximum layer coincides with that of the greatest vertical stability (Fig. 2g). The large stability is caused by the obvious halocline in the Tsushima Warm Current (G and H line), while it depends on the developed thermocline rather than halocline in the northern cold water (A, B, and C line). It has been stated that the subsurface maximum of chlorophyll contents appears at the depth where the stability of water is large (ANDERSON, 1969; TANIGUCHI, 1969; YENTSCH, 1965). A theoretical and reasonable explanation for such a distribution of chlorophyll is made by STEELE and YENTSCH (1960). Namely, they made a conclusion that a decreasing sinking rate of phytoplankton is necessary to produce chlorophyll maxima at the foot of the euphotic zone.

The depth of the maximum of the pigments concentration is shallower at Sts. H_1 and H_7 (20–30m) in comparison with that at the other stations (40–50m) of the H line. Judging from the vertical profiles of the temperature, salinity, stability, and phosphate-phosphorus (Fig. 2, e-h), it is obvious that such vertical distributions of the pigments concentration are associated with upwelling of water. The depth of the chlorophyll-a maximum layer at St. B_2 existing below the pycnocline corresponds to the depth of the second maximum layer of living diatom population. The diatom community in that layer is mainly composed of cold water species such as *Corethron histrix* and *Thalassiosira rotula* which find their preferable circumstances in the gloomy and low temperature domain (OHWADA, 1971).

(3) *Chlorophyll-a concentration and dissolved oxygen*

In the cold water area of the A, B, C, and E line, supersaturated oxygen concentrations are found in the subsurface layer which is well coincident with the

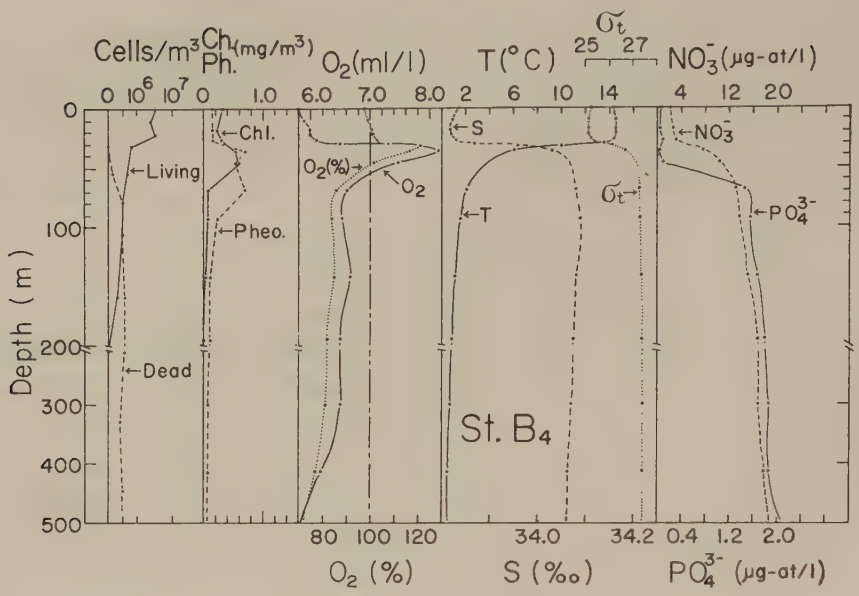

Fig. 3. Vertical distribution of total cells of diatoms, chlorophyll-a, phaeophytin, dissolved oxygen, temperature, salinity, density in situ, phosphate-phosphorus. and nitrate-nitrogen at St. B_4.

maximum layer of chlorophyll-a and the vertical stability of water (Figs. 2, 3). This phenomenon may be attributed to the integration of oxygen which is formed by active photosynthesis since the remarkable thermocline has been developted in early summer (ANDERSON, 1969). From this reason it is assumed that an active photosynthesis has been carried out in the northwestern cold water area in the Sea of Japan (Fig. 1). Such a phenomenon is also found over large area of the North Pacific Ocean during summer (KITAMURA, 1958; REID, 1962).

In the area of the Tsushima Warm Current, on the other hand, such a remarkable supersaturation of oxygen is not found. This is probably due to the fact that the accumulation of chlorophyll-a is formed in the Proper Water of the Tsushima Warm Current which originally contains deficient oxygen, and consequently, oxyen production by photosynthesis cannot afford to make supersaturation.

In spite of the high concentration of chlorophyll-a (1.4 $\mu g/l$) supersaturation of oxygen does not occur in the surface layer at St. C_1, because the produced oxygen is probably released to the air keeping balance by air-sea interaction (MIYAKE, 1965).

(4) *Living diatom population and chlorophyll-a concentration*

The living diatom populations are not always correlated with the concentration of chlorophyll-a (Table 1). Though very large numbers of living diatom cells, being

Table 1. Cell numbers of living diatoms, concentrations of chlorophyll-a, chlorophyll-a contents per one cell, dominant species of diatoms (%) in samples taken at Sts. G_3 and B_4, October, 1969.

Station	Depth (m)	Living cells/l	Ch.-a (μg/l)	Chl.-a ($10^{-6}\mu$g/cell)	Dominant species of diatoms (%)
G_3	0	61,500	0.17	3	*Chaeto.* spp. (36), *Ast. jap.* (10), *Thalassiothrix frauenf.* (40)
	10	89,000	0.14	2	*Chaeto.* spp. (34), *Ast. jap.* (16), *Thalassiothrix frauenf.* (35)
	30	217,000	0.22	1	*Ch.* spp. (21), *Ast. jap.* (10), *Thal. frauenfeldii* (46)
	50	47,900	0.34	7	*Ch.* spp. (37), *Ast. jap.* (28), *Thal. frauenfeldii* (25)
	75	6,300	0.08	13	*Asterionella japonica* (74)
	100	1,000	0.04	40	*Asterionella japonica* (44)
	200	—	0.01	—	
	300	—	0.01	—	
B_4	0	3,600	0.30	83	*Climacodium biconcavum* (95)
	20	3,300	0.29	88	*Cl. biconcavum* (90)
	30	460	0.55	1,200	*Cl. biconcavum* (100)
	50	50	0.60	12,000	*Asteromphalus heptactis* (25), *Rhizosolenia stolterfothii* (25)
	75	60	0.08	1,330	*Ast. heptactis* (40), *Rhriz. stolterfothii* (40)
	100	5	0.05	10,000	*Chaetoceros atlanticus* (100)
	200	—	0.01	—	
	300	—	0.00	—	

more than $5\cdot10^4$ cells/l, are found in 0–50m layer of St. G_3, amounts of chlorophyll-a are not so large, showing 0.14–0.34 μg/l. The diatom community in this layer is composed of very small-sized species; *Chaetoceros radicans, C. compressus, C. affinis, Asterionella japonica, Thalassiothrix frauenfeldii*, etc.

Consequently the averaged chlorophyll-a contents are 10^{-6}–$7\cdot10^{-6}$ μg/cell. On the other hand, notwithstanding the diatom population is not so large, being about $3\cdot10^3$ cells/l in 0–20m layer of St. B_4, chlorophyll-a concentrations are not so small, showing about 0.30 μg/l. The diatom community is occupied almost by large-sized

species such as *Climacodium biconcavum*. As a result, mean chlorophyll-a contents show more than ten times as large as those at St. G_3 being $83 \cdot 10^{-6}$ μg/cell.

Though the composition of diatom community at the depth of 30m at St. B_4 is not different from that of the upper water, the population decreases to 460 cells/*l*. As the results, chlorophyll-a contents of each cell increase remarkably up to $1200 \cdot 10^{-6}$ μg/cell. These results suggest adaptation of the cells to weak light. A reasonable explanation for such a cell adaptation has been given by STEELE (1964) and ANDERSON (1969).

(5) *Pycnocline and nutrient concentration of surface water*

In the northern cold waters, after the formation of the seasonal pycnocline in spring, high phytoplankton photosynthesis in the upper water reduces nutrient to undetectable concentrations; as a result, phytoplankton concentration declines and remains low throughout summer and autumn. Below the pycnocline, nutrient concentrations increase with depth and remain relatively high (Fig. 3). As the bottom of the upper mixing layer becomes deeper, the chlorophyll maximum layer may gradually deepen, leaving a zone of nutrient deficient water between it and the pycnocline. Therefore nutrients that might normally be supplied to the surface waters by diffusion and mixing from the lower layers are mostly used by the phytoplankton making up the chlorophyll-maximum zone. Thus, the pycnocline and chlorophyll maximum may act as an efficient subsurface nutrient trap over the northern cold water area, and low productivity of the surface waters appears during summer.

Acknowledgements

The author wishes to express his hearty thanks to Dr. Yutaka KAWARADA, the Japan Meteorological Agency, for his kindness that he offered the raw data of chlorophyll measurements obtained on board the R.V. *Ryofu Maru* at author's disposal. He also appreciates to the research staffs and crews on board the R.V. *Ryofu Maru*, *Kofu Maru*, *Chofu Maru*, *Shumpu Maru* and *Seifu Maru*, for their cooperation at sea.

References

Anderson, G.C. (1969): Surface chlorophyll maximum in the northeast Pacific Ocean. *Limnol. Oceanogr.*, **14**(3), 386–391.

Aruga, Y. and S. Ichimura (1968): Characteristics of photosynthesis of phytoplankton and primary production in the Kuroshio. *Bulletin of the Misaki Marine Biological Institute, Tokyo University*, **12**, 1–20.

Ichimura, S. and Y. Saijo (1959): Chlorophyll content and primary production of the Kuroshio of the southern mid-coast of Japan. *Bot. Mag. Tokyo*, **72**, 193–202.

Ichimura, S., Y. Saijo and Y. Aruga (1962): Photosynthetic characteristics of marine phytoplankton and their ecological meaning in the chlorophyll method. *Bot. Mag. Tokyo*, **75**, 212–220.

Kawarada, Y. and A. Sano (1969): Distribution of chlorophyll and phaeophytin in the western North Pacific. *Oceanogr. Mag.*, **21**(2), 137–146.

Kitamura, H. (1958): Oxygen distribution in the North Pacific Ocean, chemical oceanography in the North Pacific (IV). *Umi To Sora*, **34**, 71–75.

Koblenz-Mishke, O.J. (1960): On the study of primary production in the sea by Soviet scientists. *Internat. Hydrobiol.*, **45**, 319.

Miyake, Y. (1965): Elements of geochemistry. Maruzen Company, Ltd., Tokyo, 229–233.

Ohwada, M. (1971): Vertical distribution of diatoms in the Sea of Japan. Biological Oceanography of the northern North Pacific Ocean, dedicated to Dr. S. Motoda. (in printing)

Ohwada, M. and K. Tanioka (1971): Cruise report of the simultaneous observation in the Japan Sea in October 1969. *Oceanogr. Mag.*, **23**. (in printing)

Reid, J.L. (1962): Distribution of dissolved oxygen in the summer thermocline. *Jour. Mar. Res.*, **20**, 138–148.

Saijo, Y. (1969): Chlorophyll pigments in the deep sea. *Bull. Japan. Soc. Fish. Oceanogr.*, Special Number, 179–182.

Saijo, Y., S. Iizuka and O. Asaoka (1969): Chlorophyll maxima in Kuroshio and adjacent area. *Mar. Biol.*, **4**(3), 190–196.

Saijo, Y. and S. Nishizawa (1969): Excitation spectra in the fluorometric determination of chlorophyll-a and pheophytin-a. *Mar. Biol.*, **2**(2), 135–136.

Steele, J.H. (1964): A study of production in the Gulf of Mexico. *Jour. Mar. Res.*, **22**, 211–222.

Steele, J.H. and C.S. Yentsch (1960): The vertical distribution of chlorophyll. *Jour. Mar. Biol. Ass.*, **39**, 217–226.

Taniguchi, A. (1969): Regional variations of surface primary production in the Bering Sea in summer and the vertical stability of water affecting the production. *Bull. Facul. Hokkaido Univ.*, **20**(3), 169–179.

Yentsch, C.S. (1965): Distribution of chlorophyll and phaeophytin in the open ocean. *Deep-Sea Res.*, **12**(5), 653–666.

Yentsch, C.S. and D.W. Menzel (1963): A method for the determination of phytoplankton chlorophyll and phaeophytin by fluorescence. *Deep-Sea Res.*, **10**, 221–231.

The Oceanographical Magazine, Vol. 23, No. 1 (1971)

日本海におけるクロロフィルおよびフェオフィチンの分布

大和田　守

（舞鶴海洋気象台）

螢光光度計を用いて1969年10月日本海におけるクロロフィルおよびフェオフィチンの鉛直分布について調査した．

光合成活性のあるクロロフィルの最多層は，その分解物であるフェオフィチンの最多層と一致し，季節的に生成される密度躍層中或はそれよりも僅かに下層に存在する（密度躍層付近で植物プランクトンの沈降速度が小さくなって集積されるという説が有力）．即ち，20m から75m 層にそれらが分布する．これらの層は更に溶存酸素量の最多層（最大過飽和層）にも一致している．

クロロフィルの濃度は，そこに存在する生きている植物プランクトンの個体数とは必ずしも一致するものではない．これは，植物プランクトン群を構成している種類が各各異なり，1つ1つの細胞の大きさが異なるために，クロロフィル含有量が異なることによる．また，組成が同じであっても，有光層の下層では植物プランクトン細胞が弱光に適応してクロロフィル含有量を増すという現象も起るからである．

日本海北西部の冷水域内では，春に形成され始める躍層は夏に発達し，秋までは持続するが，この躍層が表層への営養補給の障碍となり，夏から秋にかけての表層植物プランクトンの少ない原因になっている．

The Oceanographical Magazine
Vol. 23, No. 1, pp. 33 to 45, December 1971

An STD system for instrumented buoy

Koichi NAGASAKA

Japan Meteorological Agency

(Received September 30, 1971)

Abstract: An STD (Salinity-Temperature-Depth recorder) was designed to be clamped on the mooring rope of the instrumented buoy. Separately interrogated with digitized command codes, the in situ sensors return oceanographic informations to the surface buoy with FM analogue signals. A single conductor inside the mooring rope is used as the transmission line, which is inductively linked to the sensor units.

1. Introduction

Recently the necessity of accurate information on the marine environment is rapidly increasing for many purposes, especially for improving the forecast of weather and oceanographic conditions. Collection of marine data is carried out by many types of data acquisition systems, such as research vessels, aircraft, satellites, marine platforms and instrumented buoys. Selection of a system is mainly due to the desired efficiency and allowable cost. Among those systems the buoys seem to be a very attractive and promising means. Especially it is very helpful to collect the long time-series data at a rather low cost.

Although moored oceanographic buoys have been intensively experimented for more than ten years, no standardized technique and type have been established. In addition to development of buoy itself, development of reliable sensors is a must for successful automatic data buoy. By our buoy experiences sensors for oceanographic information pose more difficult problems than those for meteorological information. As our first attempt, a kind of STD system to be mounted along a mooring rope of an anchored buoy was designed. The project mainly aimed to develop a new technique to transfer signals between a surface buoy and in situ sensors and interrogate those sensors from the buoy. In this report the description of the instrumentation and the result of measurement in the sea are presented.

2. System configuration

Temperature and salinity are the most important parameters of oceanographic conditions. To observe these variables easily several kinds of STD (Salinity-Temperature-Depth recorder) have recently been put on the market. Continuous profiles of salinity and temperature as function of depth are obtained merely by lowering the instrument from vessel. The technique to detect those physical parameters seems to be fairly well developed. However, such kind of instruments are designed to be operated aboard research vessels. Therefore, the ordinary STD is not successfully introduced to the buoy system by being attached along the mooring cable. Aside from the requirement of the greater reliability than that of the ship born type STD, how to control in situ sensors and how to transmit the obtained information signals to the bouy are essential problems to not only the STD but also the other instruments for automatic data buoy system.

The usual way to transfer the signals between underwater sensors and the surface buoy is shown in Fig. 1 (A). Multiconductors corresponding to the number

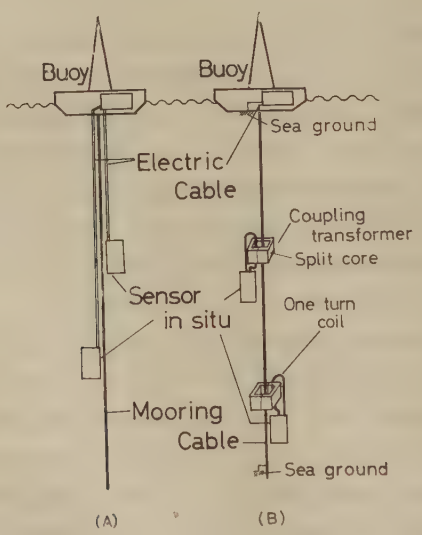

Fig. 1. Hard-wire method (A) and inductive coupling method (B).

of in situ sensors are employed and connected to the sensors by water-proof connectors. This is means which is called hard-wire method. The hard-wire method

seems to be very simple to transmit electrical signals. However, from a point of view of the buoy technology this method has the following disadvantages.

(A) The number of conductors increases with the number of sensors.

(B) The water-proof connectors and multi-conductor water-tight cable are expensive and breakable.

(C) It is difficult to set a sensor on the mooring rope at a desired depth; this seems to be a decisive shortcoming.

Consequently the hard-wire method is unreliable and unapplicable, when the large number of sensors are required. Even though a single conductor is used, the faults except the first one still remain. To eliminate those above-mentioned problems, the development of new technique has been expected. The inductive coupling method as shown in Fig. 1 (B) is adoped for this purpose. This method is commonly used in the multi-communicate telephone system and also applied to the clamp-on ammeter. The possibility of appling the method to couple the underwater sensors to the transmission line had been already demonstrated by U.S. NOR. This not only removes the need of any mechanical connectors but also makes it possible to put sensors at any desired depth. Moreover if multi-conductor cable is used, it becomes possible to switch over to the other spare conductor at the top of cable, when insulation of a conductor becomes poor or/and a conductor is broken. The rope that contains conductor inside the strand is on the market in Japan.

In addition to the inductive coupling method, the new type interrogation method to control the underwater sensors is also adopted to the STD system.

(2-1) *The summary of design requirements*

The requirements in designing the STD system in this experiment are summarized as follows;

(A) The system is capable of continuing the reliable observations eight times a day for more than six months.

(B) The measurement is made by the interrogation from the control unit in the surface buoy.

(C) The fairly large number, more than thirty, of sensors are able to be commanded and to be clamped on a mooring rope.

(D) The range and accuracy of measurement of the each sensor is;

(a) Salinity; 32— 36‰ ±0.03‰

(b) Temperature; 0— 30°C ±0.1 °C

(c) Depth; 0—500m ±0.5% of the indicated value

(E) The sensor is capable of being mounted at any desired depth on a mooring cable.

(2-2) *Principle of operation*

The instrument is composed of the four blocks; a control unit, an insulated

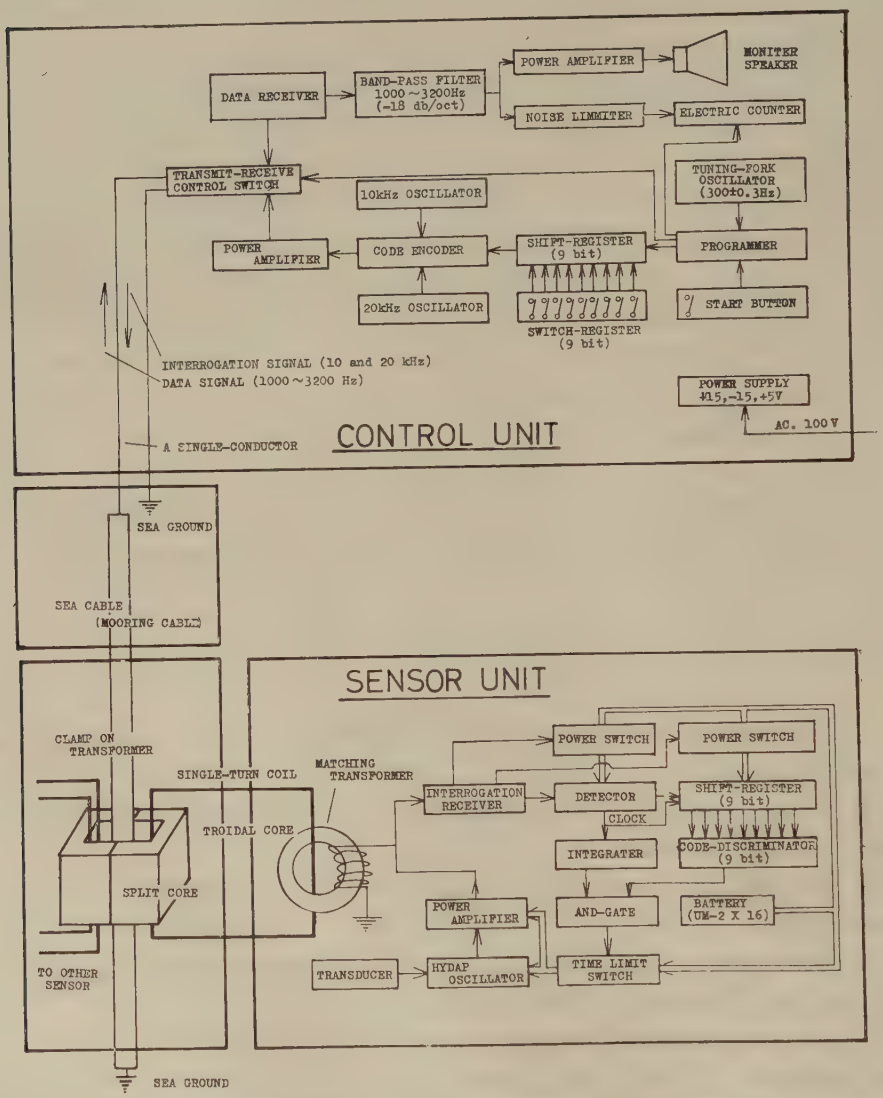

Fig. 2. Block diagram of STD system for an instrumented buoy made in this experiment.

cable, a clamp-on transformer and three in situ sensors (STD). The sensors are independently interrogated and return the observed parameters. The block diagram is shown in Fig. 2. The principle of the operation of the instrument is as follows.

When one of the sensors is required to send the oceanographic information to the surface buoy, the 9 bit call-sign assigned to the disired sensor is deposited in the switch-register. The stored code is sent to the shift-register by pushing the start button. The shift-register converts the 9 bit parallel signal into the time series signal to control the gate of the call-sign encorder. The gate pass a 20 KHz or 10 KHz signal generated by the two oscillators to the power amplifier for 0.7ms, corresponding to the '1' or '0' bit of the call-sign code. The gate also gives a blank signal for 0.7 ms. between the bit, then the bit rate of the call-sign signal is 75 pcs. Before and after the 9 bit code, 6 bit 10 KHz leader and 20 KHz trailer codes are also made by the encorder. The typical form of the interrogation signal is shown in Fig. 3. Here the time-sequence of the control unit is controled by the program-

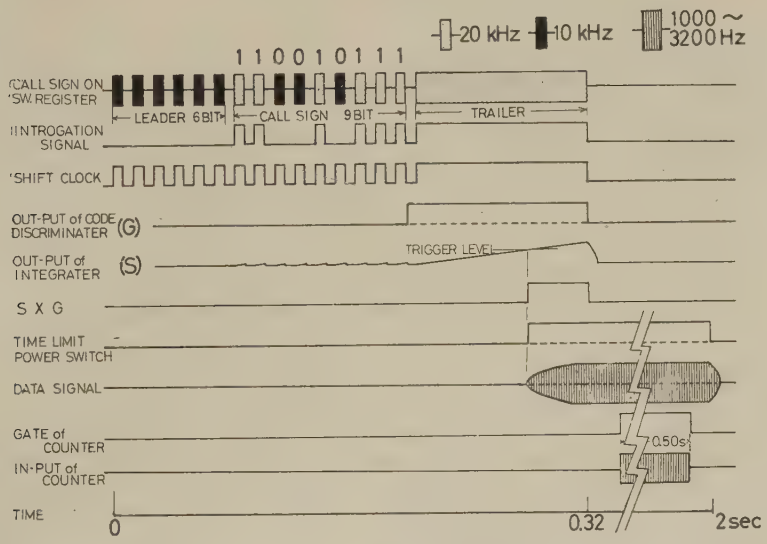

Fig. 3. A typical wave form of interrogation signal and time-sequence of the system.

mer which is drived with clock pulse generated by the fork-tuning oscillator. The output of the power amplifier is sent to the sea cable through the transmission-receive control switch. The interrogation signal is led to the secondary windings of the transformer whose core is clamped around the sea cable. The

sensor unit has an interrogation receiver that is always operated with very small power to detect the induced signal. The leader code of the interrogation signal turns on the detector, resister and discriminater circuits in the sensor units. The detecter circuit generates '1' or '0' bit code corresponding to the frequency of call-sign signal and they are stored at the switch-register. The code discriminator compairs the incoming code with the code assigned to the sensor. Only when the code assigned to a sensor coincides with the incoming one, the time-limit switch can be turned on after the trailer code is detected by the integrater. Then the sensing circuit and power amplifier are energized for the next 1.7 sec. and the other sensors wait the next interrogation. The interrogated sensor observes the physical variable and sends the information to the control unit with a FM analogue signal. The receiver in the control unit amplifies the reply signal. After eliminating noise and triming the amplitude of the signal, the FM analogue information is digitized by the electric counter. Finally the observed variable is indicated in three decimal figures.

(2–3) *The outline of the electronic circuits*

The specification of the circuits is summarized in Table 1. The all of electronic packages are put together with solidstate parts. Here the explanation is limited to the particular circuits of the system.

Table 1. The specification of electronic design.

(A) Control unit		
(1)	The maximum number of sensors	512 sets
(2)	The minimun time interval between each sampling	2 sec
(3)	The bit rate of the interrogation signal	75 bps
(4)	The frequency of the interrogation signal	10 and 20 KHz
(5)	The out-put power of the interrogation signal	8 W
(6)	The pass band frequency of the filter	1000~3200 Hz, −18db/oct
(7)	The gate time of the frequency counter	0.500 sec
(8)	The requirement of electric power; usually	10 W
	; during interrogation	15 W
(B) Underwater sensor		
(9)	The frequency of data signal	100~3200 Hz
(10)	The requirement of electric power; usually	480 μW
	; during receiving the interrogation	200 mW
	; during measurement	480 mW

(A) The interrogation method

Though the principle of this part was described in the previous section, digital codes as the interrogation signals can be emphasized. In the STD system of the MONSTER BUOY, a pair of tone signals is used as an interrogation signal. The method needs the large number of tone generaters to control the many underwater sensors in the control unit and also the large number of tone sensitive reed relays in the underwater packages, Moreover, the frequency of a tone generater has to be correctly identical with that of resonance of reed relay. The interrogation system adopted in this experiment is capable of controling the extremely large number of sensors with a very simple and rough interrogater. The present system can control 512 ($=2^9$) sensors. Owing to the recent remarkable progress in digital circulit technique developed for electric computors, shift-registers and other components used in this instrument are reliable and inexpensive.

(B) Detector of each variable.

Sea-water salinity is determined by measuring electrical conductivity with an inductive coupling cell as ordinary STD. Salinity is expressed in a function of temperature, conductivity and pressure of sea-water. A special circuit to compensate the effects of temperature and pressure is employed in the salinometer. Temperature transducer is a platinum resistance thermometer. A potentiometer driven by bouldon-tube pressure gauge is used as a pressure transducer. The same type pressure transducer and three thermisters are also used as the compensater in the salinity transducer. The parameters sensed with such transducers are converted into FM signals whose frequencies are proportional to the physical variables by the Hydap Oscillators developed by Tsurumi Seiki Co., Ltd. (US PAT. No. 3581238).

(C) Inductive coupling method and cable

In the experiment 500m long cabtyre cable was tentatively used as the sea cable. The resistance of a conductor is 1.4 ohms/km. The cable is electrically connected to sea-water at the bottom end. The connection is made by a sheet of aluminum whose dimension is $200 \times 200 \times 1$ m/m. The control unit is also linked to the sea-water near the sea surface by the same manner.

Fig. 4 shows the detail of the inductive coupling part. The principle of this part is essentially similar to that of transformer. The core of the transformer clamped around the sea cable is of split type. The magnetic pathlength and cross section of the core are 270m/m and 700mm^2 respectively. Its permeability is more than 4000. This split core enables to clamp the sensors at any desired depth on a cable. This is the final reason to introduce the inductive coupling

method to the system inspite of the low efficiency.

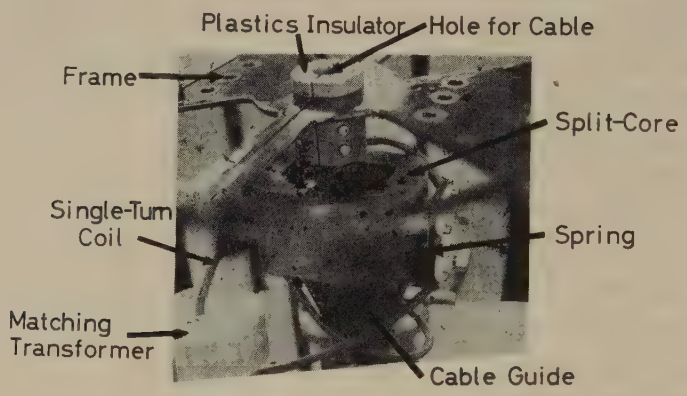

Fig. 4. Details of clamp-on sensor system.

Besides the coupling transformer, an another transformer is put not only to improve the matching of the impedance between the single turn coil and the sensor unit but also to connect them without any water proof plug. The troidal core and the secondary winding of the matching transformer are mounted inside a troidally shaped pressure tight case made of plastics at the top of each sensor (Fig. 4). The space around the cores is surrounded with seawater so that it also acts as single turn coils. But the resistance of the sea-water coil is about 10 ohms and extremely larger than that of the single turn coil whose impedance is estimated approximately 0.03 ohms at 2 KHz. Therefore the effect of the seawater around the cores is negligible from the viewpoint of transfering signals.

(D) Power source of sensor and control units

The large effort has been made to decrease the electric power to drive the underwater units. The power requirement for each underwater unit is supplied by sixteen standard D-Cell (UM-2) 1.5 volt flashlight batteries, whose rated power is more than 50 WH under the same condition to the operation. The total amount of the electric power required to operate as many as thirty sensors every three hours for six months is approximately 30 WH. If the more powerful batteries were used, it would be possible to operate for one year without replacing and/or recharging batteries. The control unit requires about 500 WH for six months. This power is supplied from the ship's line source of 100 volt AC in the experiment.

(2–4) *Mechanical design*

The mechanical configuration of the device is shown in Fig. 5.
The dimension and weight of each unit are as follows;
The control unit $520 \times 250 \times 470$ m/m 17.5 Kg

(A)

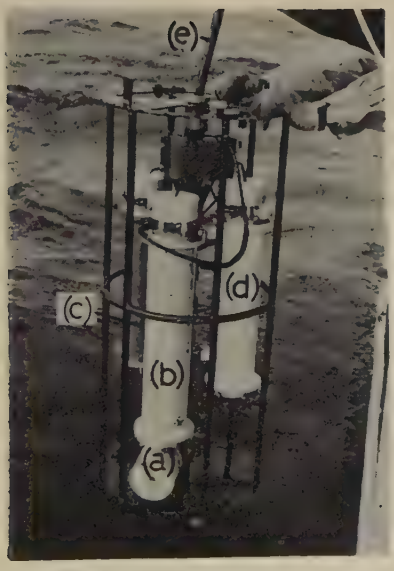

(B)

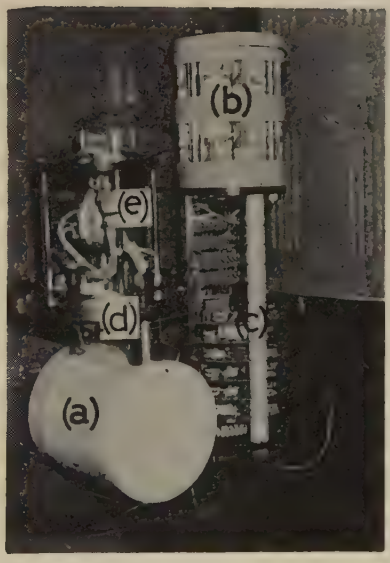

(C)

Fig. 5. (A) control unit.
(B) underwater unit; (a) salinometer cell, (b) salinity sensor, (c) depth sensor, (d) temperature sensor, (e) sea cable.
(C) inside view of the salinity sensor; (a) salinometer cell (b) batteries, (c) electronic part, (d) thermister, (e) pressure guage.

The electric counter (Takeda Riken TR-3735)	200×149×350 m/m	6.5 Kg
The underwater unit	950×460 Φ m/m	55 Kg (in air) 45 Kg (in water)

The each sensor unit is housed in a stainless-steel pressure tight case to withstand the hydrostatic pressure at 100m depth. The three sensors (STD) are guarded by a steel frame as shown in Fig. 5 to prevent the mechanical damage. The frame consits of two semi-cylindrical cages hinged on each end and is clamped to the rope with cable guide fastend with ten pieces of bolts. The two pieces of the split core push each other with springs not to make a large gap between them. Plastics insulator is used at the end of the cable guide of the steel frame so that the frame does not act as a single turn coil around the core. The detail of this part is shown in Fig. 4. The present experiment mainly aimed to investigate the problems associated with the inductive coupling method and the interrogation system. Antifouling of the underwater package was not taken into consideration.

3. Trial operation in the sea

The field test of the instrument was carried out in the Sagami Bay (35°30′N, 139°20′E) and the Sea of Japan (39°46′N, 134°20′E) in March and May in 1971 respectively. The underwater package was attached on a cable paid out from the Ryofu Maru instead of clamping on a mooring rope of an instrumented buoy and the control unit was on board the ship. The system worked perfectly as expected even if the sensor units were lowered about 500m from sea surface. It was possible to give the command of measurements under the condition that the resistance of 100 ohms was seriesly added to the sea cable. The impedance of the sea cable was ranged from 100 to 200 ohms at 10 KHz with the various length of the cable in the water from 100 to 500 m. Significant difference in the power loss between the control unit and the sensors was not recognized even though the way of grounding was changed from a 200 × 200m/m aluminum plate to the hull of the ship. This means the plate is effective in the present purpose.

Example of continuous measurement by this instrument is given in Fig. 6, which was made in the Sea of Japan. The result of Nansen bottle cast taken at the same time during the operation is also shown in Fig. 7. Comparing these two, the agreement between them is satisfactorily good for the temperature. The disagreement in the salinity seems to be due to the long stabilization time of the

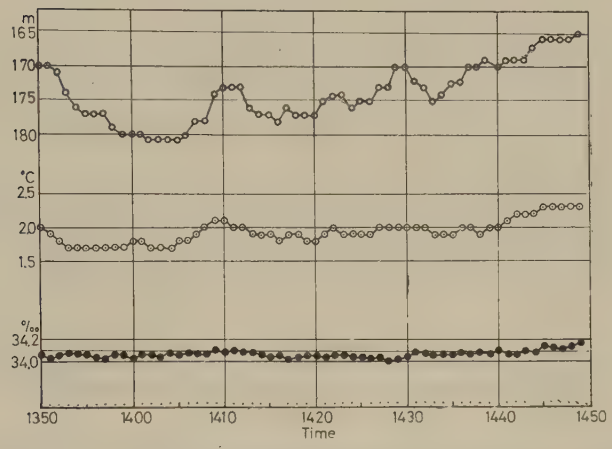

Fig. 6. An example of measurement with the STD system.

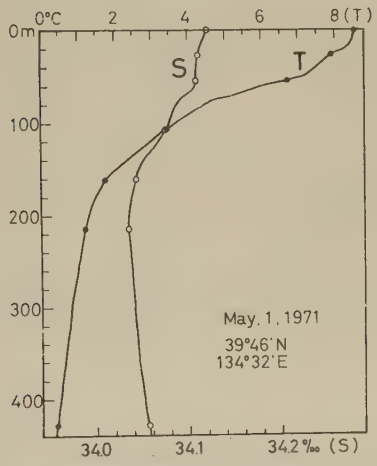

Fig. 7. The result of Nansen bottle casts taken at same time to the example shown in Fig. 6.

sensor oscillator. The oscillator was designed to have a warming up time less than 1 sec. However, one of the oscillators had the longer warming up time. The precise study of the accuracy of the instrument could not carried out because of the time shortage.

4. Conclusion

The conclusion of this experiment is summarized as follows.

(A) The usefulness of the inductive coupling technique was well confirmed. The technique is able to be applied for the other oceanographic instrumentation, such as current meters.

(B) The digitized interrogation system was perfectly operated as expected. The each in situ sensor replied to the interrogation without failure. However, it is desirable to ensure the measurements by commanding sensors twice at every observation.

(C) The function of the sensors was almost satisfactory. The error of each measurement was apporoximately within the magnitude assigned by the specification of the instrument.

(D) The stabilization time of the sensor oscillator has to be decreased as short as possible. The shorter the time is, the smaller the electric power to drive the system becomes.

(E) The endurance test has not be done. The life test of the dry cell and electronic package are important subjects in shore laboratories. The antifouling was not taken into consideration in the present study. However, the marine fouling is the primary difficulty foreseen in the long term operation of underwater sensors, especially sensors for the salinity. The fouling changes rapidly the cell constant and results in extremely large errors. Development of new antifouling technique is expected.

(F) The frame of sensors package was successful. The easier way to clamp the package on a rope should be developed in the future study.

5. Acknowledgement

The author is grateful to members of the scientific parties, officers and crew aboard the Ryofu Maru, Japan Meteorological Agency for their cooperation. He also indebted to Drs. I. IMAI and J. MASUZAWA in Marine Division, JMA for their constant interest and encouragement for this project. This work was sponsored by the Science and Technology Agency as a part of the project to develop the buoy technology.

ブイ用STDの試作

長坂昂一

（気象庁・海洋気象部）

海洋・気象観測用ブイの係留ロープに取付け，海水の塩分・水温及び深度を計かる測器を試作した．装置は，ブイ本体に収められる制御部，塩分・水温・深度を計測する海中受感部，単芯の伝送ケーブル，ケーブルと海中受感部とを接続する電磁結合部の四部から，構成されている．

海中受感部は，制御部からの指令により，各々の計測を行い，その値を周波数信号に変換する．制御部では，この信号の周波数を計数し，計測結果をデジタル表示する．

ケーブルと受感部との接続には，従来用いられている耐水プラグによらず，両者を鉄芯により電磁的に結合する方法をとった．この方法によれば，ケーブルと鉄芯とを単に鎖交させるのみで両者を接続できるため，受感部をケーブル上の任意の所に取付けることができ，ブイ設置点の海況に応じてセンサーの深度を変えることができる．

制御部から海中受感部への計測指令には，10 KHz 及び 20 KHz の信号の組合せによる 9 bit のデジタル符号を各受感部に割当て，そのセンサー特有の呼出符号の対してのみ応答計測するようにした．この方式では，非常に簡単な指令装置で多数（512台）のセンサーを制御できる．

海中受感部は，乾電池により半年間（3時間毎の計測）動作できる．

海中受感部の計測範囲は 0～30°C, 30～36‰, 0～500m，その精度は ±0.1°C, ±0.02‰, ±5% である．

昭和47年2月26日　発行

編集兼
発行者　気象庁
東京都千代田区大手町1の3の4

印刷者　藤原秀雄

印刷所　昌美印刷株式会社
東京都千代田区神田錦町3の16